Scaling of slope, upslope area, and soil water deficit: Implications for transferability and regionalization in topographic index modeling

Nawa Raj Pradhan,[1] Fred L. Ogden,[1] Yasuto Tachikawa,[2] and Kaoru Takara[3]

Received 15 November 2007; revised 27 May 2008; accepted 15 September 2008; published 16 December 2008.

[1] Development of a generally applicable rainfall-runoff model and identification of associated model parameters require understanding of connections between physical processes at disparate scales and hydrological similarities between catchments. In this study, we test the hypothesis that understanding of geomorphometric scaling relations can reduce uncertainty when transferring model parameters between catchments when applying the TOPMODEL concept. Scaling relations on contributing area, slope, and contour length were successfully used to scale the topographic index distribution in watersheds located in vastly different regions of the world: Japan, Nepal, Panama, and the United States. Model parameters were identified through calibration of TOPMODEL in the 210-km^2 Kamishiiba catchment in Japan. These parameters were transferred to two Sun Koshi River subcatchments in Nepal, namely, the 850-km^2 Likhu and 620-km^2 Balephi catchments, the 414-km^2 Upper Rio Chagres catchment in Panama, and the 37-km^2 Town Brook catchment in the United States. Results show how a priori estimates of the most sensitive model parameters can be used to make predictions in poorly gauged or ungauged basins with some degree of confidence provided that scale effects are considered. This result hints at the potential universality of the topographic index distribution scaling relations in catchments where runoff is dominated by subsurface flow.

Citation: Pradhan, N. R., F. L. Ogden, Y. Tachikawa, and K. Takara (2008), Scaling of slope, upslope area, and soil water deficit: Implications for transferability and regionalization in topographic index modeling, *Water Resour. Res.*, *44*, W12421, doi:10.1029/2007WR006667.

1. Introduction

[2] Many river basins in the world are either ungauged or poorly gauged. The prediction of flow in those rivers is an important task for the management of water resources. In most regionalization studies, a relationship between the parameters of the model and the catchment descriptors is developed [*Parajka et al.*, 2005], so that the parameters are transferable to similar regions [*Blöschl*, 2005]. A lack of reliable methods to translate the spatial, and also temporal, scale dependence relations into effective hydrological model parameters poses a serious problem [*Kavetski et al.*, 2003; *Pradhan et al.*, 2006] that hampers predictions in ungauged basins of developing countries, where the information gained from one scale is to be used in making predictions at other (usually coarser) scales [*Pradhan et al.*, 2006]. This is due to the fact that coarsening of the resolution of spatial data sets results in the loss of information at higher spatial frequencies [*Kuo et al.*, 1999], leading to significant errors in simulation results, owing to strong nonlinearity in the scale-dependence effect on many hydrological processes.

[3] One issue that hampers generalized topographically driven saturation-excess modeling is that the topographic index is dimensional, having units of ln(L). This dimensionality dictates that topographic indices developed for the same catchment using DEMs with different resolution will not be identical. Hence, the topographic index distribution is not scale invariant to underlying data resolution. Overcoming this problem requires development of scaling relations.

[4] Thus, scale transformation and scale invariance appear as fundamental steps for developing a process-based method to identify similarities between catchments and for the development of an effective regionalization technique. The problem of transferring information gained at one scale for making predictions at a different hydrological scale is a scaling problem [*Beven*, 1995].

[5] In this study, we test the hypothesis that geomorphometric scaling relations may be used to transfer model parameters between catchments where saturation-excess runoff is dominant. Testing of this hypothesis could assist in the development of an approach for a transferable rainfall-runoff model and transferable model parameters to assist predictions in ungauged basins using a freely available global data set. Development of a transferable rainfall-runoff model and the identification of transferable model parameters are key steps in establishing similarities and connections among physical processes at disparate scales and in the determination of possible linkage of hydrological

[1] Department of Civil and Architectural Engineering, University of Wyoming, Laramie, Wyoming, USA.
[2] Hydrology and Water Resources Engineering Laboratory, Department of Urban and Environmental Engineering, Kyoto University, Kyoto, Japan.
[3] Disaster Prevention Research Institute, Kyoto University, Kyoto, Japan.

0043-1397/08/2007WR006667$09.00

Table 1. Effective Parameter Values for the Saturation Excess Runoff Generation Mechanism of TOPMODEL Identified at 50-m DEM Resolution in the 210-km^2 Kamishiiba Catchment

Parameter	Value
Lateral transmissivity of soil at saturation condition, T_o (m^2 h^{-1})	9.8
Decay factor of lateral transmissivity with respect to saturation deficit, m (m)	0.07
Maximum root zone storage, Rz_{max} (m)	0.001

similarities between catchments making scale transformation and scale invariance the fundamental requirement.

[6] Section 2 presents the study objectives, methodology, watersheds and data. In section 3 we discuss the scale dependence of the TOPMODEL state variables. In sections 4–6, we discuss the scale dependencies of dominating geomorphometric parameters and development of methods to accurately account for the effect of scale in upslope catchment area, slope, unit contour length, and topographic index. The effectiveness of our approach is demonstrated in section 7 by testing whether the modeling outcome is reliable at a scale that is significantly different from the scale where the model was calibrated, without recalibration. Discussion and conclusions follow in section 8.

2. Objectives, Methods, Watersheds, and Data

[7] In this study we examine the utility of scaling relations for transferring geomorphometric model parameters between scales and basins for the saturation-excess TOPMODEL, and is motivated by the need to make predictions in ungauged basins. The objective of this study was to test the hypothesis that detailed consideration of the impact of scale on model parameters will also improve transferability of topographic-index-derived parameters between different catchments. This hypothesis is tested by transferring TOPMODEL parameters identified by calibration in the Kamishiiba catchment in Japan, shown in Table 1, to two subcatchments of the Sun Koshi river in Nepal, the Upper Rio Chagres catchment in Panama, and the Town Brook catchment in the northeastern United States.

2.1. TOPMODEL Formulation Used in This Study

[8] The TOPMODEL formulation used in this study is essentially the same version of TOPMODEL in wide distribution today. Section 3, represents the overland flow and base flow in the TOPMODEL formulation used in this study. Calibration of TOPMODEL was first performed on runoff volume. Muskingum-Cunge channel routing was added to the simulation of the Kamishiiba catchment only after the TOPMODEL parameter set in Table 1 was identified. Rainfall on a saturated grid is the overland flow to be routed. Routing improved simulation results at the catchment by increasing the Nash-Sutcliffe coefficient in comparison with observed hydrographs. The addition of channel routing had no other effect on the simulation results, as there is no feedback in this formulation between the channel and runoff generating components of TOPMODEL.

[9] Given the high-quality data set from Kamishiiba catchment, we selected to use it for parameter estimation in this regionalization study. *Pradhan et al.* [2006] identified the parameters in the Kamishiiba catchment adopting trial and error approach in the calibration. *Pradhan et al.* [2006] derived an estimate of the parameter m in the Kamishiiba catchment from the first-order hyperbolic function that fitted the recession curve obtained from the observed discharge of rainfall [*Ambroise et al.*, 1996]. Prior estimation of the m parameter also helped to identify the set of calibrated parameters that is rather less affected by equifinality [*Beven*, 2006] in calibration.

2.2. Study Watersheds

[10] Our study uses calibration data from the Kamishiiba catchment in Japan, and tested the utility of scaling relations for improved regionalization using data from two tributaries of the Sun Koshi River in Nepal, the Upper Rio Chagres in Panama, and Town Brook in New York, United States. These watersheds are discussed in the following sections.

2.2.1. Kamishiiba Catchment, Japan

[11] This study uses a research-quality data set from the 210-km^2 Kamishiiba catchment, which is located in Japan. This same data set was used by *Pradhan et al.* [2006] to validate the scaling relations employed in the present study. The Kamishiiba catchment lies in Kyushu Island of Japan. Kyushu, the southernmost of the four major islands of Japan, has a mountainous interior, is subtropical and remains warmer throughout the year than other parts of Japan. The summer months are hot and humid with high rainfall intensity. The mean annual rainfall in the Kamishiiba catchment is approximately 2000 mm. Since the simulations of the Kamishiiba catchment were done in the warmest season, snow processes were not simulated.

2.2.2. Likhu and Balaphi Catchments, Nepal

[12] The two basins used in Nepal are the 850-km^2 Likhu and 620-km^2 Balaphi catchments. Nepal, with an area of 147,181 km^2, has more than 6000 rivers stretching from the Himalayas to the southern plain. This dense river network flows through steep topography. Approximately 80% of the 2000–3500 mm total annual rainfall is concentrated in the relatively short monsoon season [*Gyawali*, 1989], which lasts approximately 4 months [*Japan International Cooperation Agency*, 1985]. These peculiar characteristics lead to a set of hazards, including frequent floods and debris flows. Although there are some gauging stations installed in some rivers, many river basins in Nepal are either ungauged or poorly gauged. The lack of understanding of the scale-dependence relations into effective hydrological models has up to now posed a serious problem for making predictions in ungauged basins in developing countries. Often in this case, either only coarse-resolution DEM data are available or the information gained at fine scale is to be used in making predictions at coarser scales.

[13] The Likhu and Balaphi catchments are tributaries of the Sun Koshi River in Nepal. The Sun Koshi basin has steep terrain and monthly average relative humidity rising up to 80% during the rainy season. Humidity in the dry season, on the other hand, varies widely during a 1-day period and is typically much lower than of the rainy season. The rainfall data used in Likhu and Balaphi catchments are the daily rainfall data from the nearest available gauging stations. Precipitation gauging stations number 1224 and 1103 were used for estimating rainfall over the Likhu catchment. In the Balaphi catchment, data were used from precipitation gauging stations number 1006, 1008, 1009, and 1103. Rainfall-runoff data were obtained from the

Department of Hydrology and Meteorology, Government of Nepal. For both the Likhu and Balaphi catchments, evaporation data used were obtained from climatological records of Nepal (see http://www.dhm.gov.np/index.php?p = publication). Four climatological seasons can be identified in Nepal [*Nayava*, 1980]. The pre–monsoon season (March–May) is characterized by hot, dry weather with scattered rainfall; toward the end of this period, it becomes more humid with thundershowers. The summer monsoon season (June–September) is governed by the southeasterly flow of moisture-laden air from the Bay of Bengal. The post–monsoon season (October–November) has a typical onset date coincident with the autumnal equinox. Rainfall activity is substantially reduced with November typically the driest month. The winter season (December–February) is generally dry, although westerly weather systems may bring cold air and winter precipitation (in the form of snow) that contributes to low-flow regimes of these rivers. Groundwater is primarily recharged by the monsoon rainfall, and is the most significant contribution to low-flow regimes of these rivers in Nepal. Some portions of these catchments lie above the snow line; however, it is very difficult to clearly distinguish meltwater contributions due to the overwhelming influence of the summer monsoon rain [*Hannah et al.*, 2005]. For these reasons, snowmelt was not considered an important process in these catchments.

2.2.3. Upper Rio Chagres Catchment, Panama

[14] The Greater Panama Canal Watershed is a hydrologically complex and ecologically diverse. The watershed consists of a mix of pristine old-growth forest managed as national park, and partly deforested grazed areas in 13 subbasins. There are two significant reservoirs in the greater Panama Canal watershed [*Harmon*, 2005]. The Rio Chagres, notable as the only river in the world to flow into two oceans, is the largest river by annual flow volume entering into the Panama Canal and provides approximately half the water required for operating the canal while comprising only a third the area of the greater Panama Canal watershed. The 414-km^2 Upper Rio Chagres is a protected National Park. As such it is predominantly covered by old-growth forest, less than 10% of the watershed disturbed by human activities.

[15] Panama is located in the seasonal tropics, with pronounced wet and dry seasons. Typically, precipitation peaks during June–July and October–November when the intertropical convergence zone passes across the region, with very little rain falling during the dry season between January and March. Rainy season storms generated in the Caribbean tend to track from north to south, so that there is a pronounced N–S precipitation gradient across the Panamanian isthmus. The Atlantic coastal region receives an annual average of >3000 mm of precipitation as compared to <2000 mm for the Pacific coastal region on the leeward side of the continental divide although the year-to-year variations in total precipitation can be significant. For example, annual precipitation in the Upper Rio Chagres watershed is quite variable, with annual values ranging from 1,800 to 3,200 mm between 1972 and 2005. It never snows in the Rio Chagres catchment.

2.2.4. Town Brook Catchment, New York

[16] The 37-km^2 Town Brook catchment lies in Catskill mountains in southern New York State. In humid, well-vegetated areas, such as in the northeastern United States, most direct runoff is generated by the saturation-excess mechanism, that is, via precipitation on or exfiltration from saturated areas in the landscape [*Ward*, 1984]. Runoff generation in Town Brook and adjacent watersheds was examined by *Lyon et al.* [2004] and *Steenhuis et al.* [1995]. The Town Brook catchment is smaller and significantly different from the other catchments used in this study. While the catchments in Japan, Nepal, and Panama are relatively young as a result of geologically recent tectonic or volcanic activity, the Town Brook catchment is in the northern Appalachian province, which is geologically much older than the other study catchments.

2.3. DEM Data Sources

[17] DEM data at 1000- and 90-m resolutions for the catchments in Nepal and Panama were downloaded from Global 30 Arc-Second Elevation (GTOPO30) and Shuttle Radar Topography Mission (SRTM) data sets from the United States Geological and Survey (USGS) EROS data center web site, respectively. The 50-m resolution DEM for the catchments in Japan was obtained from Geological Survey of Japan (GSJ). The DEM at 10- and 30-m resolution for Town Brook catchment in the United States were obtained from National Elevation Data set (NED), United States Geological and Survey (USGS) Web site.

3. Effect of DEM Resolution on Saturated Area and Base Flow Predictions From TOPMODEL

[18] The topographic index distribution for the 210-km^2 Kamishiiba catchment was calculated using a 50-m resolution DEM. TOPMODEL was calibrated using rainfall-runoff data from this catchment, which resulted in Nash-Sutcliffe efficiency, hereafter referred to as N–S efficiency, of 94%. The corresponding identified value of lateral soil transmissivity parameter was 9.8 m^2/h (see Table 1). Figure 1a shows the model predicted that 7% of the catchment area was saturated at the initial time step.

[19] When a 1000-m DEM was used to develop the topographic index distribution and the model parameters identified through the original calibration were applied, the initial percentage of saturated area predicted by TOPMODEL increased to 59% as shown in Figure 1b. This is quite an unreasonable prediction for a conceptual state variable owing to the change in DEM resolution, and highlights the problem with the dimensionality of the topographic index. This very large error in the TOPMODEL-predicted discharge results in a negative N–S efficiency as a consequence of the overestimation of the saturated area. Furthermore, the base flow predicted by the TOPMODEL using the topographic index distribution derived from the 1000-m DEM is very small compared to 50-m DEM resolution TOPMODEL as shown in Figure 2. This is attributable to the fact that too much water is stored in the soil as demonstrated by the 52% overprediction of the saturated area.

[20] This overprediction of saturated area is primarily caused by the effect of DEM resolution on the topographic index distribution [*Zhang and Montgomery*, 1994]. Figure 3 shows the scale effect in the cumulative topographic index distribution using topographic data from catchments in different parts of the world. In the TOPMODEL framework,

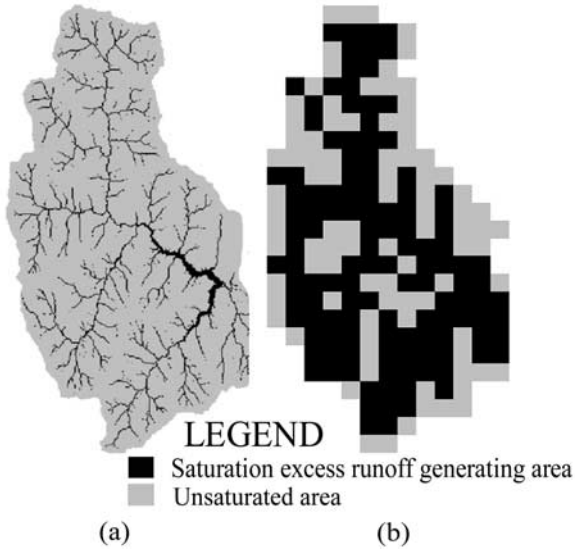

Figure 1. Analysis of distributed saturated area output of TOPMODEL at different digital elevation model (DEM) resolutions in the 210-km^2 Kamishiiba catchment in Japan using model parameters identified using 50-m DEM resolution in the Kamishiiba catchment. (a) The 7% saturated area is predicted by TOPMODEL at the initial time step, when 50-m DEM resolution is used. (b) The 59% saturated area is the output of TOPMODEL at the initial time step, when 1000-m DEM resolution is used.

the topographic index is used to distribute the local saturation deficits, given knowledge of the mean storage deficit [*Beven and Kirkby*, 1979]. The topographic index [*Kirkby*, 1975] of TOPMODEL is defined as

$$TI = \ln\left[\frac{a}{(\tan\beta)}\right], \tag{1}$$

where a is the local upslope contributing area per unit contour length [L] and β is the slope angle of the ground surface [L L^{-1}].

[21] Equation (2) is the relation between $\overline{S}(t)$ [L], the spatial mean storage deficit and S (i, t) [L], local saturation deficit at each location i in a catchment as [*Beven and Kirkby*, 1979]

$$S(i,t) = \overline{S}(t) + m\left[\left(\overline{TI} - TI\right) + \left(\ln T_o - \overline{\ln T_o}\right)\right], \tag{2}$$

where T_o [L^{2}T^{-1}] is the local value of lateral (horizontal) transmissivity when the soil has zero storage deficit; $\overline{\ln T_o}$ is the catchment average of ln T_o; m is a decay factor of saturated transmissivity of soil with respect to saturation deficit with dimensions of length [L]; and $\overline{TI}$ is the catchment average of the topographic index.

[22] Areas with S (i, t) ≤ 0 in equation (2) represent contributing areas for saturation excess overland flow as shown in Figure 1. Considering an effective T_o value, the local saturation deficit is totally controlled by local topographic index and the catchment average of the topographic index. The effect of DEM resolution on the cumulative topographic index distribution as shown in Figure 3 is the reason for the different predictions of saturation shown in Figure 1 as given by equation (2).

[23] In the TOPMODEL framework, subsurface contributions to streamflow, $Q_b(t)$ [LT^{-1}] can be derived from equation (2) as

$$Q_b(t) = T_o e^{-\overline{TI}} e^{-\overline{S}(t)/m}, \tag{3}$$

which is also controlled by the catchment average of the topographic index. The DEM resolution effect on the topographic index shown in Figure 3a is the reason for the difference in subsurface flow shown in Figure 2 as given by equation (3).

[24] The scale dependence of the topographic index with decreasing resolution is caused by the loss of high spatial

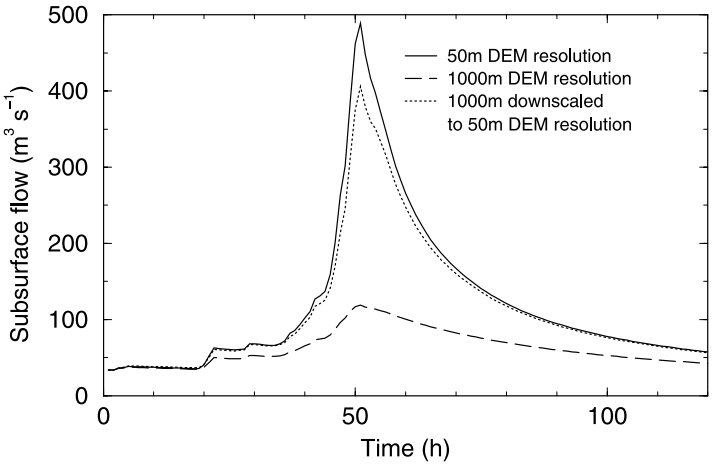

Figure 2. Comparison of subsurface flow obtained from 50-m DEM resolution TOPMODEL, 1000-m DEM resolution TOPMODEL, and TOPMODEL applied at 1000-m DEM resolution with scaled topographic index to 50-m DEM resolution. The applied effective parameters are identified by 50-m DEM resolution TOPMODEL. A rainfall event 6 days in duration (22 September 1999 to 27 September 1999) in the 210-km^2 Kamishiiba catchment in Japan was used to analyze the subsurface flow.

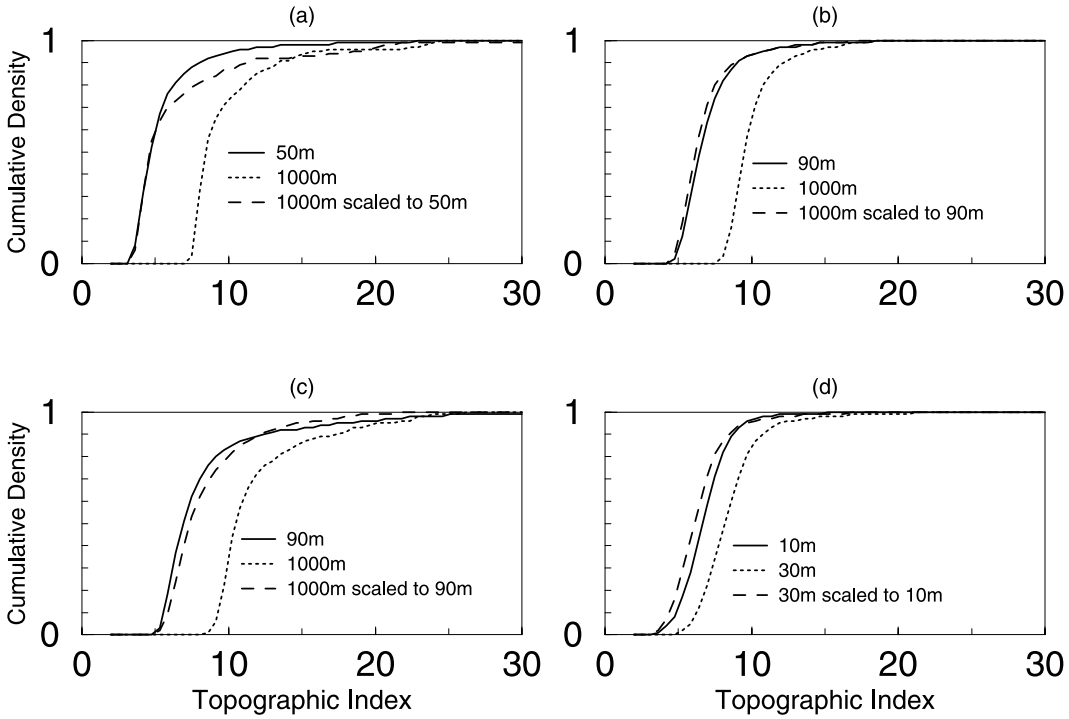

Figure 3. DEM resolution effect on density distribution of topographic index and applicability of the topographic index distribution scaling method in different topographic regions of the world: (a) 210-km^2 Kamishiiba catchment in Japan, (b) 850-km^2 Likhu catchment in Nepal, (c) 414-km^2 Upper Rio Chagres catchment in Panama, and (d) the 37-km^2 Town Brook catchment in the northeastern United States.

frequency components in the upslope catchment area, and the underestimation of the slope when using a coarse-resolution DEM. The error in the predicted saturated state variable and base flow response can be removed by scaling the topographic index distribution from the available scale to another scale of interest [*Pradhan et al.*, 2006]. Understanding the scaling of the topographic index can only be obtained by deriving a scaling formulation of the dominant geomorphological parameters like upslope catchment area, unit contour length and slope.

4. Scaling Solution to the Effect of DEM Resolution on Geomorphometric Information

[25] Scaling relations for upslope contributing area and slope developed by *Pradhan et al.* [2006] are showed in this section. This section also introduces a new method to produce an unbiased measure of unit contour length that is independent from DEM resolution.

4.1. Scaling of Local Upslope Contributing Area and Slope Angle

[26] Many physically based models of hydrological and geomorphic processes rely on spatially distributed characterization of drainage area and slope angle. *Pradhan et al.* [2006] showed when upslope catchment area is calculated at fine resolution, information is lost when the calculation is repeated using coarse-resolution DEMs. *Pradhan et al.* [2006] also showed that slopes are underestimated when using coarse-resolution DEMs. To avoid this scaling effect, which can seriously affect the accuracy of hydrological and geomorphological models, *Pradhan et al.* [2006] successfully derived the scaling formulation for the upslope catchment area and slope–angle. The scaling method for upslope contributing area derived by *Pradhan et al.* [2006] is defined as

$$A_{i,scaled} = \left\{ \frac{A_i}{N_s e^{\left[\frac{(1-N_i)H_N}{N_o}\right]}} \right\}, \tag{4}$$

where the suffix i is a location in a catchment, A_i is the upslope catchment area obtained from a coarse-resolution DEM, $A_{i,scaled}$ is the scaled upslope catchment area at a point i, N_s is the total number of desired target fine-resolution grids included in an available course-resolution grid, N_i is the number of the coarse-resolution grids contained in the upslope contributing area at a location i in the catchment, N_o is the number of the coarse-resolution grids contained in the upslope catchment area at the outlet of the catchment, and H_N is a factor [*Pradhan et al.*, 2006].

[27] The method for scaling local land-surface slope developed by *Pradhan et al.* [2006] is defined as

$$\theta_{i,scaled} = \alpha_{i,steepest} d_{i,scaled}{}^{(1-D_i)}, \tag{5}$$

where i is the central grid location in 3 × 3 moving window pixels, $\theta_{i,scaled}$ is the downscaled steepest slope in 3 × 3 moving window pixels, $d_{i,scaled}$ is the steepest slope distance of the target-resolution DEM, D_i is the fractal dimension, and $\alpha_{i,steepest}$ is a coefficient.

[28] *Pradhan et al.* [2006] found that equation (4) works for any range of scaling provided that there are enough

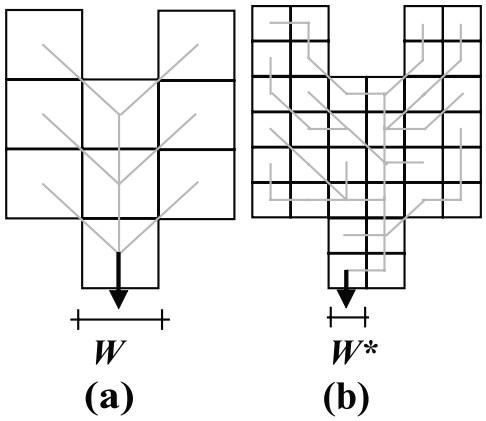

Figure 4. Scale effect on the conceptual derivation of contour length. (a) Unit contour length representation of a coarse-resolution DEM. (b) Unit contour length representation of a fine-resolution DEM.

pixels of a grid size to represent the distribution in a catchment. In equation (5), slope is a function of the measurement scale by assuming that topography is unifractal in a specified range of measurement scale. This unifractal concept can break down at very fine scales limiting the scaling range as shown by *Pradhan et al.* [2006].

4.2. Development of a Method for Scaling Contour Length in the Topographic Index

[29] With coarse DEM grids, the simple use of either the single-flow direction method or multiple-flow direction method overestimates the contour length near the catchment divide compared with estimates developed from fine DEM grids. With fine DEM grids, the simple use of either the single-flow direction method or multiple-flow direction method underestimates the contour length in the vicinity of the catchment outlet when fine-resolution DEM is used compared with that from coarse DEM grids. For example, at the outlet, the upslope drainage area is the same (Figures 4a and 4b), but the contour length representation of a coarse-resolution DEM, W, in Figure 4a is larger than the contour length representation of a fine-resolution DEM, W^*, in Figure 4b.

[30] To solve the scale problem in defining the contour length using the single-flow or multiple-flow direction method, contour length is varied from the target fine-resolution grid at the catchment divide region to the available coarse-resolution grid at the catchment outlet. The downscaled contour length is defined as

$$W_{i,scaled} = \frac{W_i}{R_f I_f}, \tag{6}$$

where $W_{i,\ scaled}$ is the scaled contour length from the available coarse-resolution DEM to the target fine-resolution DEM at location i, W_i is the unit contour length of the available coarse-resolution DEM at location i, and I_f is the influence factor per unit contour length. R_f is resolution factor defined as

$$R_f = \frac{Coarse\ \ DEM\ \ Resolution}{Target\ \ DEM\ \ Resolution}. \tag{7}$$

As contour length is varied from the target fine-resolution grid at the catchment divide region to the available coarse-resolution grid at the catchment outlet, the influence of R_f on W_i must gradually decrease in equation (6) from value 1 at the catchment divide portion to $\frac{1}{R_f}$ as W_i becomes larger. For this reason, in equation (6) the influence factor I_f is introduced having the value 1 at the catchment divide portion so that the unit contour length given by a target fine-resolution grid is obtained, having value $\frac{1}{R_f}$ at the outlet so that unit contour length is defined by the available coarse-resolution DEM. Using exponential decay, the influence factor is equal to 1 at the catchment divide and transitions to a value of $\frac{1}{R_f}$ at the catchment outlet as the upslope catchment area increases. Thus I_f is defined as

$$I_f = e^{\left[\frac{(1-N_i)H_R}{N_o}\right]}, \tag{8}$$

where N_i is the number of the coarse-resolution grids contained in the upslope contributing area at a location i in the catchment and N_o is the number of the coarse-resolution grids contained in the upslope catchment area at the outlet of the catchment. Considering that the influence of R_f on W_i in equation (6) is almost negligible at the outlet of the catchment, where $N_i = N_o$ and $I_f = \frac{1}{R_f}$, the value of H_R introduced as a factor in equation (8) can be obtained from equation (8) by substituting $N_i = N_o$ and $I_f = \frac{1}{R_f}$ as

$$H_R = \frac{N_o}{N_o - 1} \ln R_f. \tag{9}$$

[31] Equations (6) and (8) give a scale-independent method of representing unit contour length as

$$W_{i,scaled} = \left\{ \frac{W_i}{R_f e^{\left[\frac{(1-N_i)H_R}{N_o}\right]}} \right\}. \tag{10}$$

The differences in the mathematical formulation for upslope catchment area in equation (4) and unit contour length in equation (10) is that equation (4) uses N_s and H_N whereas equation (10) uses R_f and H_R.

5. Development of a Scaling Approach in Hydrogeomorphology

[32] Substituting the value of a and β in equation (1) by $\frac{A_{i,scaled}}{W_{i,scaled}}$ from equations (4) and (10) and $\theta_{i,scaled}$ from equation (5), the downscaled topographic index, TI_{scaled} is defined as

$$TI_{scaled} = \ln\left(\frac{\frac{A_i}{N_s e^{\left[\frac{(1-N_i)H_N}{N_o}\right]}}}{\frac{W_i}{R_f e^{\left[\frac{(1-N_i)H_R}{N_o}\right]}} \theta_{i,scaled}} \right). \tag{11}$$

Substituting $N_s = R_f^2$ [*Pradhan et al.*, 2006] in equation (11) and simplifying, the downscaled topographic index, TI_{scaled} is defined as

$$TI_{scaled} = \ln\left(\frac{A_i e^{\left[\frac{(1-N_i)(H_R-H_N)}{N_o}\right]}}{W_i \theta_{i,scaled} R_f} \right). \tag{12}$$

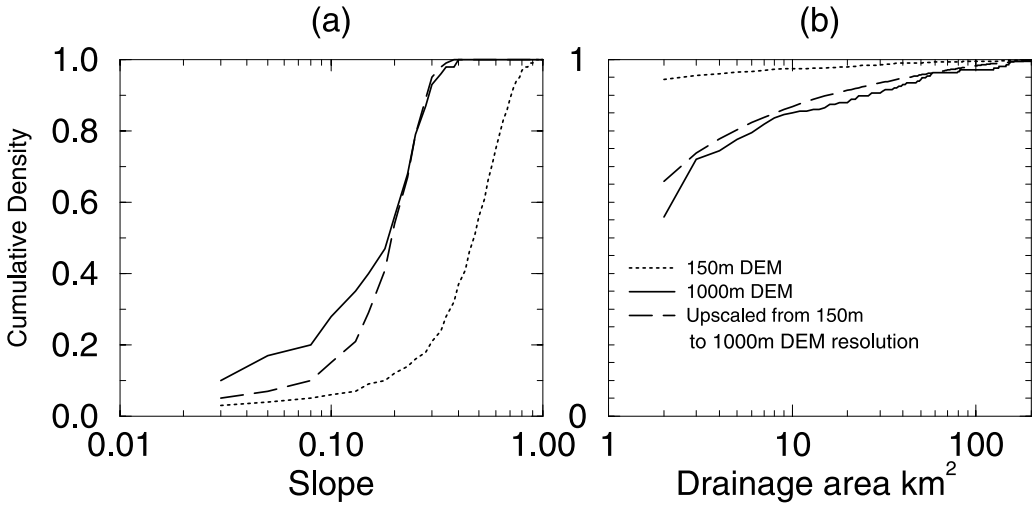

Figure 5. Upscaling slope and catchment area in the 210-km^2 Kamishiiba catchment. (a) Distribution functions of steepest slope obtained from different DEM resolutions and upscaled slope. (b) Distribution functions of upslope catchment area obtained from different DEM resolutions and upscaled upslope catchment area.

Substituting the value of TI in equation (1) with the value of TI_{scaled} from equation (12) in equation (2), the scaled local saturation deficit is defined as

$$S(i,t) = \overline{S}(t) + m \cdot \left\{ \left[\overline{TI}_{scaled} - \ln\left(\frac{A_i e^{\left[\frac{(1-N_i)(H_R-H_N)}{No}\right]}}{W_i \theta_{i,scaled} R_f} \right) \right] + \left(\ln T_o - \overline{\ln T_o} \right) \right\}, \quad (13)$$

where $\overline{TI}_{scaled}$ is the catchment average of TI_{scaled} in equation (12).

[33] Substituting the value of $\overline{TI}$ by $\overline{TI}_{scaled}$ in equation (3) the scaled base flow is defined as

$$Q_b(t) = T_o \quad e^{-\overline{TI}_{scaled}} e^{-\overline{S}(t)/m}. \quad (14)$$

Equations (13) and (14) are used to produce scale-independent saturated area and base flow response in TOPMODEL framework.

6. Upscaling and Downscaling

[34] Equations (7), (8), (10), (12), (13), and (14) are explained from the downscaling point of view. Thus in explaining the derivation of these equations, a coarse-resolution DEM is taken as an available DEM and a fine-resolution DEM is taken as the target-resolution DEM at which the geomorphometric information is to be obtained. Applying equation (12), to scale the cumulative topographic index distribution developed from a coarse-resolution DEM shows a close fit with the topographic index at a fine-resolution DEM in Figure 3. Figure 3 shows the applicability of the scaling method of topographic index distribution in watersheds located in vastly different regions of the world.

[35] Applying equation (13), the saturated area obtained dropped down from 59% in Figure 1b to 10%, very close to that obtained using 50-m DEM resolution in Figure 1a. Thus by scaling the topographic index distribution and applying equation (14), it is shown in Figure 2 that the similar base flow response as that of 50-m DEM TOPMODEL is obtained from the 1000-m DEM resolution TOPMODEL without recalibrating.

[36] In this paper we applied the upscaling relations for slope and upslope contributing area published by *Pradhan et al.* [2006] for the first time to make predictions in diverse catchments. To upscale, we simply replaced the fine-resolution DEM with a coarse-resolution DEM to which the geomorphometric information is to be upscaled. Thus while upscaling, R_f in equation (7) is defined as

$$R_f = \frac{Available \quad Fine \quad DEM \quad Resolution}{Target \quad Coarse \quad DEM \quad Resolution}. \quad (15)$$

Thus, R_f in equation (15) is less than 1 while upscaling. When upscaling, R_f used in all the scaling relations is defined by equation (15) and N_s is the square of the R_f defined by equation (15) and N_i and N_o are defined at a fine-resolution DEM. Furthermore, while upscaling, $\theta_{i,scaled}$ in equation (5) is the upscaled steepest slope in 3 x 3 moving window pixels and $d_{i,scaled}$ is the steepest slope distance of a target coarse-resolution DEM. While upscaling the slope, values of $\alpha_{i,steepest}$ in equation (5) are derived directly from the steepest slope of the available fine-resolution DEM.

[37] Figure 5a shows the upscaled slope distribution function from 150- and 1000-m DEM resolutions. The RMS error between the cumulative distribution of slope from 1000- and 150-m DEM resolutions in Figure 5a is 0.342. The RMS error between the upscaled cumulative distribution of slope from 150-m DEM resolution to 1000-m DEM resolution and the slope at 1000-m DEM resolution in Figure 5a is 0.015. Thus by the use of the slope upscaling relation, the RMS error was reduced by 95%.

[38] Figure 5b shows that the frequency distribution of upslope contributing area from 1000-m DEM resolution agrees quite well with the upscaled upslope catchment area frequency distribution from 150-m DEM resolution to the

target 1000-m DEM resolution. Without the use of the upscaling relations, the RMS error in dimensionless (0–1) upslope contributing area was 0.36%. The RMS error of the upscaled dimensionless contributing area was 0.04%. The use of the upscaling relation reduced the RMS in contributing area by 89%.

7. Tests of Improved Model Parameter Transferability by Accounting for Scale Effects on Geomorphometric Parameters

[39] This section describes our test of the hypothesis that geomorphometric scaling relations can be used to improve the transfer of rainfall-runoff model parameters between catchments where saturation-excess runoff is dominant. These tests involved calibrating TOPMODEL on the Kamishiiba catchment in Japan, and using the derived scaling relations to transfer those parameters to catchments in Nepal, Panama, and the United States. In the following sections, downscaled TOPMODEL means downscaling equations (12), (13), and (14) to a target fine-resolution scale using an available coarse-resolution DEM and upscaled TOPMODEL means upscaling equations (12), (13), and (14) to a target coarse scale using an available fine-resolution DEM.

7.1. Transferring the Model Parameters From Kamishiiba Catchment in Japan to Sun Koshi Basin Subcatchments in Nepal

[40] Similar to the Kamishiiba catchment, the Likhu and the Balephi catchments experience high humidity in summer and comparatively lower humidity in winter. The defined catchments in Japan and Nepal have tectonic activity and are geologically young mountains. The mountainous setting in both the regions in Japan and Nepal creates rivers that have steep channel slopes. Thus, there are possibilities that the parameter values obtained at the Kamishiiba catchment in Japan are applicable to the subcatchments of the Sun Koshi basin in Nepal.

7.1.1. Tests on the 850-km^2 Likhu Catchment, Nepal

[41] The Kamishiiba-calibrated parameters were applied in the Likhu catchment represented by a digital terrain model of resolutions of 1000 m and 90 m. To match the scales of model application, equations (12), (13), and (14) are applied to scale the topographic index, soil water deficit variable, and base flow.

[42] Figure 6a shows the simulated discharge when the Kamishiiba-calibrated parameters were applied at 1000-m DEM resolution in Likhu catchment. The N–S efficiency is negative. Figure 6c shows the simulated discharge of downscaled TOPMODEL from 1000-m DEM resolution to 50-m DEM resolution in the Likhu catchment with the Kamishiiba-calibrated parameters. The N–S efficiency increased from a negative value in Figure 6a to 81% in Figure 6c.

[43] Figure 6b shows the simulated discharge when the Kamishiiba-calibrated parameters were applied at 90-m DEM resolution in Likhu catchment. The N–S efficiency is 72%. Figure 6d shows the simulated discharge of downscaled TOPMODEL from 90-m DEM resolution to 50-m DEM resolution in the Likhu catchment with the Kamishiiba-calibrated parameters. The N–S efficiency increased from 72% in Figure 6b to 82% in Figure 6d.

[44] The identical simulation results are shown in Figures 9c and 9d, demonstrating that the derived scaling relations are effective in transferring the parameters identified at a fine scale to different coarse scales at which the model is applied. At this point the utility of the downscaling method presented in this research is quite clear. Reduction of the grid size also means a considerably increase in the work involved in data collection and processing [*Vázquez et al.*, 2002].

7.1.2. Tests on 620-km^2 Balephi Catchment, Nepal

[45] Figure 7 shows a long-term simulation result, from 1991 to 1996 on the Balephi catchment in Nepal. This simulation result was obtained by scaling the TOPMODEL parameters from the 1000-m original DEM to 50-m DEM resolution and applying the Kamishiiba-calibrated parameters. As catchments in Nepal are ungauged or poorly gauged, Balephi catchment discharge data for the years 1993 and 1995 are missing. Thus the simulation results for the years 1993 and 1995 in Figure 7 are blind predictions. The saturation information simulated at the end of previous years, that is year 1992 and year 1993, was given as initial state variables in those blind prediction years 1993 and 1995. The N–S efficiencies for 1991, 1992, 1994, and 1996 are 78%, 88%, 67%, and 70%, respectively, with an average of 75%.

7.2. Tests on 414-km^2 Upper Rio Chagres Catchment, Panama

[46] TOPMODEL is used in the humid tropics, and studies have shown that it performs well when the catchments are in high-moisture states [*Campling et al.*, 2002; *Molicova et al.*, 1997]. Using data provided by the Panama Canal Authority, we calibrated TOPMODEL at 90-m DEM resolution in the Upper Rio Chagres catchment, 414 km^2, in Panama, which is located at 9°N in the seasonal tropics. Figure 8 shows the TOPMODEL simulation output from January to September 1986. In Figure 8a, the calibrated top-ranked parameter set gave a N–S efficiency of 50%. Reasons for not achieving a higher efficiency could be the inabilities of TOPMODEL to take account the variety of runoff generation processes and the importance of deep groundwater in producing base flow in this tropical catchment [*Niedzialek and Ogden*, 2005] as well as the lack of detailed spatial description of rainfall data. Regional generalizations strictly require that the various processes of runoff generation acting in these regions should be carefully examined [*Pilgrim*, 1983]. We tested the transferability of the TOPMODEL parameters from the Kamishiiba catchment to the Upper Rio Chagres catchment. Given that direct calibration of TOPMODEL yielded a N–S efficiency of 50%, we would not expect the best performance of the transferred parameters to exceed this value.

[47] Figure 8b shows the simulated discharge when the Kamishiiba-calibrated parameters were applied at 1000-m DEM resolution in the Rio Chagres catchment. In this case the N–S efficiency was negative, −20%. Downscaling of the TOPMODEL parameters from 1000- to 50-m DEM resolution in the Upper Rio Chagres catchment with the Kamishiiba-calibrated parameters gave the simulation results shown in Figure 8c, where the N–S efficiency increased to 45%. Figure 8c nearly matches the simulation results in Figure 8a, which were achieved by direct calibration. Despite the fact that the TOPMODEL formulation is

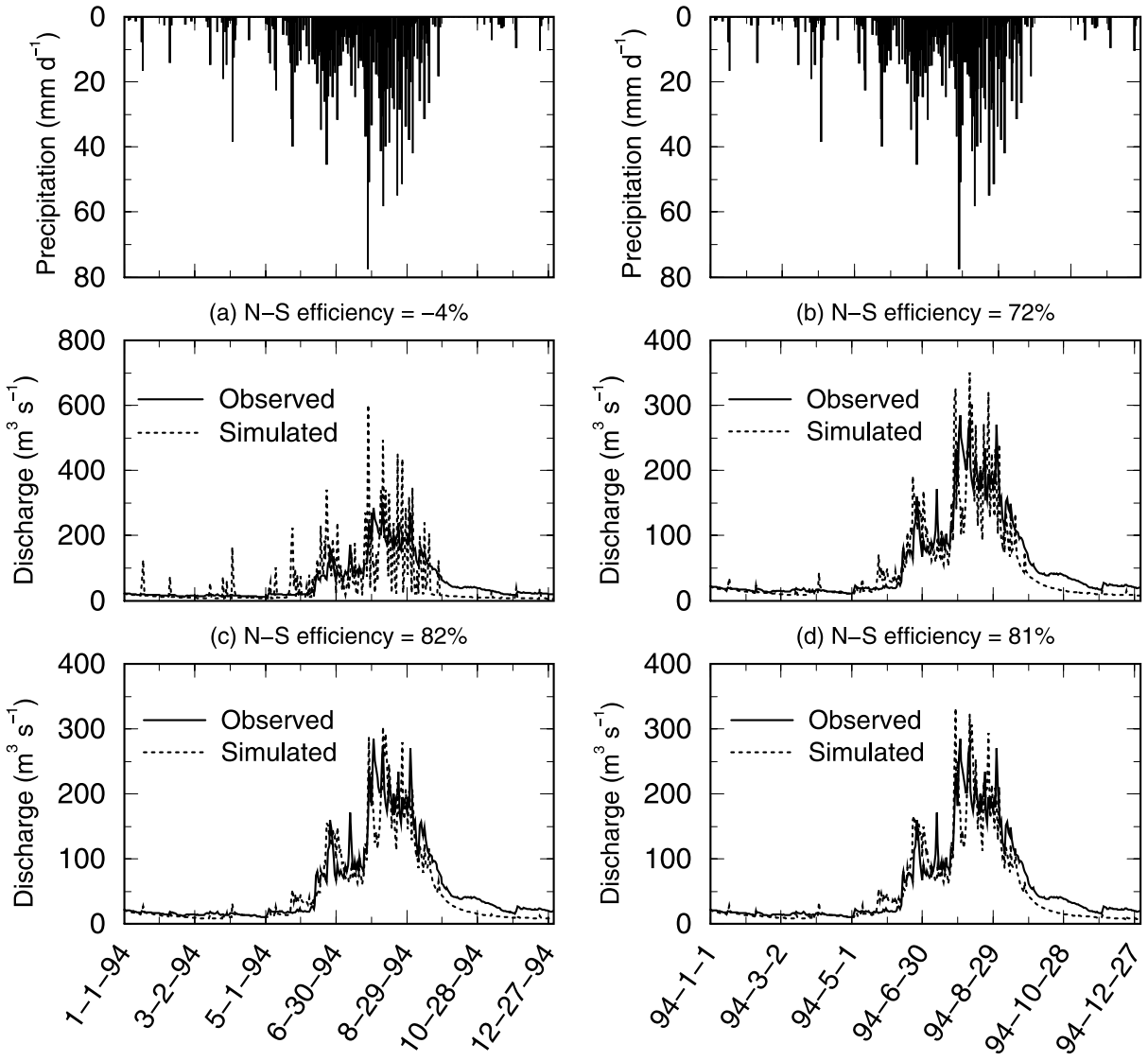

Figure 6. Comparison of TOPMODEL predictions at different DEM resolutions, with and without scale correction in 850-km^2 Likhu catchment in Nepal. All simulation results are for the same period of rainfall using basin-specific topographic index distributions and the Kamishiiba-calibrated parameters: (a) 1000-m DEM resolution, (b) 90-m DEM resolution, (c) 90-m DEM resolution scaled to 50-m DEM resolution, and (d) 1000-m DEM resolution scaled to 50-m DEM resolution.

incomplete in this watershed, as indicated by the relatively low N–S efficiency, the scaling relations presented in this study result in model performance using the scaled and transferred Kamishiiba catchment parameters that is nearly equal to that seen with direct calibration.

7.3. Tests on the 37-km^2 Town Brook Catchment, New York

[48] Figure 9 shows the TOPMODEL simulation result for the year 2003 using daily rainfall-runoff data from the 97-day period beginning in September to the first week of December, in the Town Brook, catchment in New York State, United States. Figure 9a shows the simulated discharge when the Kamishiiba-calibrated parameters were applied without scaling at 10-m DEM resolution in the Town Brook catchment resulting in a N–S efficiency of 31%. Using the scaling relations to transfer the Kamishiiba parameters from 50- to 10-m DEM resolution increased the N–S efficiency to 50% in Figure 9b. Although, the scaling relations increased the N–S efficiency from 31% to 50%, we found that TOPMODEL performed better in this catchment with recalibration at 10-m DEM itself. So in this case, given the significant difference in catchment size, the scaling relations do not explain all of the variation.

[49] To further explore this, the TOPMODEL was calibrated on the Town Brook at 10-m DEM resolution, resulting in T_o = 3.0 m^2/h and m of 0.02, and a N–S efficiency of 86%. The prior estimate of the m parameter from the first-order hyperbolic function that fitted the recession curve obtained from the observed discharge of rainfall in the Town Brook catchment was found to be 0.015 which is very close to the calibrated m value of 0.02 in the catchment. Using the Kamishiiba T_o value, and upscaling the

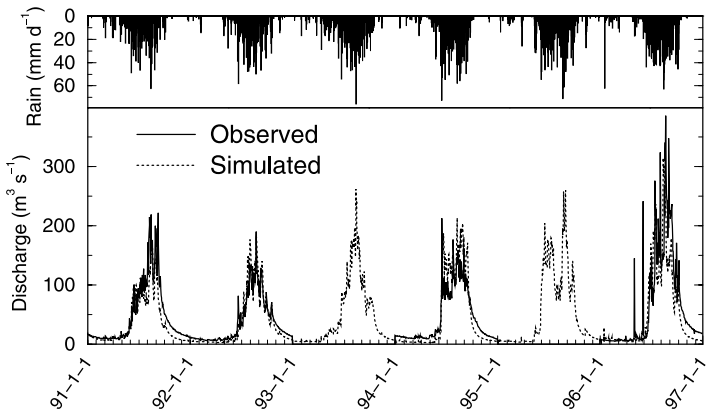

Figure 7. Long-term simulation in Balephi (Nepal) catchment at 1000-m DEM resolution and topographic index distribution scaled to 50-m DEM resolution with the Kamishiiba-calibrated parameters. Simulations for years 1993 and 1995 are blind predictions as the corresponding years have no available observed data.

TOPMODEL from 10- to 50-m DEM resolution, with the calibrated Town Brook m parameter, the N–S efficiency was 84% in Figure 9c.

8. Discussion

[50] The use of routing increased the N–S efficiency in the Kamishiiba catchment, as it did when the Kamishiiba calibration parameters were transferred to the Nepal catchments. However, the incorporation of routing but did not improve the simulation performance in the Upper Rio Chagres and Town Brook catchments. The most likely reason for this is that the response time of the 414-km^2 Upper Rio Chagres and the 37-km^2 Town Brook catchment is less than the 1-day model time step employed in this study. This paper does not consider the effect of model time step on parameter identification. This is a limitation of our study. However, the scaling relations tested in our study did improve model performance using the Kamishiiba parameters to almost equal those obtained using direct calibration.

[51] We demonstrate that accounting for grid-size scale effects improves model performance in regionalization tests. We did not seek to answer the question "is there an optimal grid size." As found by *Andrle and Abrahams* [1989] and *Klinkenberg and Goodchild* [1992], unifractal scaling of slope breaks down at very fine scales owing to different processes that control microtopography. This prevents application of equation (5) for downscaling to scales at which microtopography is important. This limits the applicability of our approach to scales on the order of a few meters to a few tens of meters.

[52] In this study, the value of the lateral transmissivity $T = 9.8$ m^{2}h^{-1} identified in calibration on the Kamishiiba, Japan, catchment was found to be applicable to some degree in all four test catchments. We cannot draw any conclusion from this result. However, *Nimmo* [2007] analyzed 64 macropore flow data sets and found that flow velocities in macropores and fractures are well bounded, with a mean value of 13 md^{-1}. An argument posed by *Brutsaert* [2008] from analysis of river recession data proposed that there is a fundamental geomorphological control wherein stream drainage density develops to produce a characteristic drainage timescale or "storage half life" of 45±15 days. The quest for fundamental hydrological variables as a result of ecological, geological or other controls is an area of active research.

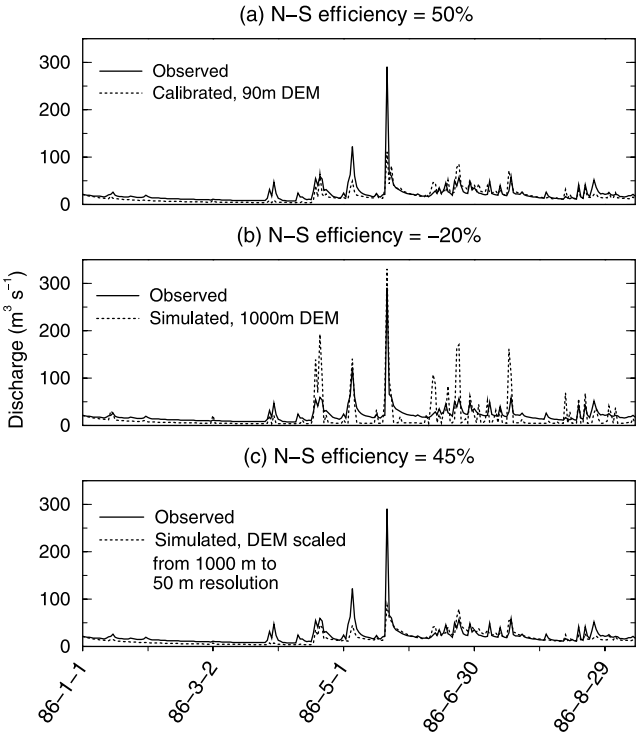

Figure 8. Transferability of parameters with scaled topographic index in the upper Rio Chagres catchment in Panama. All simulation results are for the same rainfall period (January to September 1986). (a) TOPMODEL-calibrated discharge at Shuttle Radar Topography Mission 90-m DEM resolution. (b) TOPMODEL-simulated discharge with Global 30 Arc-Second Elevation 1000-m resolution DEM using the Kamishiiba-calibrated parameters. (c) Simulated discharge with 1000-m topographic index scaled to 50-m DEM resolution using the Kamishiiba-calibrated parameters.

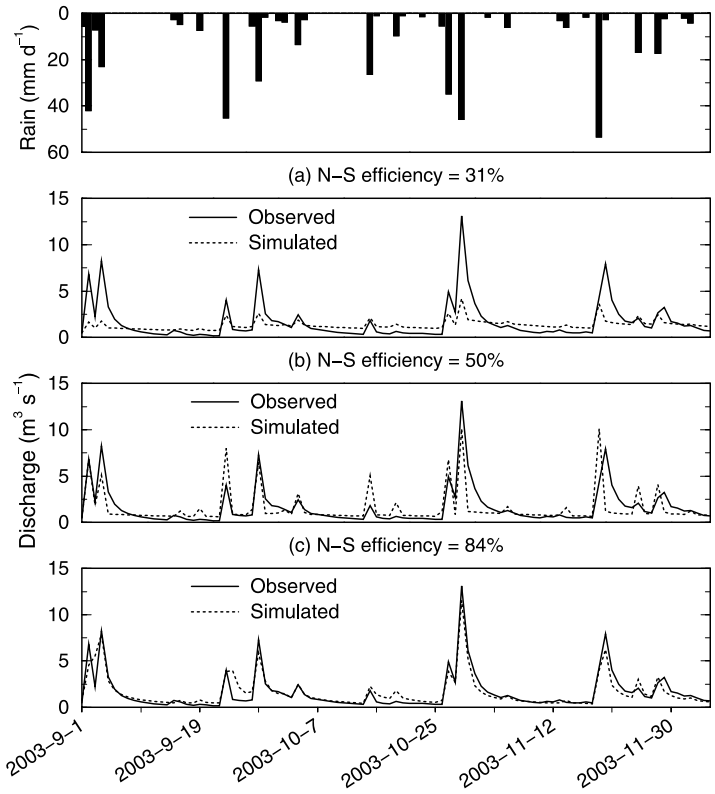

Figure 9. Transferability of parameters with scaled topographic index in the 37.1-km^2 Town Brook catchment, in the northeastern United States. (a) TOPMODEL-simulated discharge with 10-m DEM resolution using the Kamishiiba-calibrated parameters, (b) simulated discharge with topographic index upscaled from 10- to 50-m DEM resolution using the Kamishiiba-calibrated parameters, and (c) TOPMODEL-simulated discharge with upscaled topographic index from 10-to 50-m DEM resolution with the Kamishiiba-calibrated T_o value and the Town Brook–calibrated m value.

[53] In hydrologic modeling, fine-resolution DEM offers advantages over course-resolution DEM for identifying grid-resolution depended effective parameter values like the lateral soil transmissivity T [*Pradhan et al.*, 2006]. Finer-resolution DEMs allow for better description of small-scale topographic features such as low-order channels and hillslopes. Identifying a grid size for a faithful landscape representation is a future research work.

9. Conclusions

[54] The topographic index is dimensional. At a point, it is derived from local upslope contributing area, unit contour length and slope. Available methods to quantify the topographic parameters drainage area, contour length per unit area, and slope, are influenced by DEM grid resolution. This makes the topographic index at a point dependent on grid resolution. Subsequently TOPMODEL parameters that work in one watershed at one grid resolution will not work in the same basin at a different grid resolution. Knowledge of how to correct for this effect allows transfer of TOPMODEL parameters not only from one grid size to another, but also from one basin to another. Scaling relations on contributing area, slope, and contour length were successfully used to scale the topographic index distribution in watersheds located in vastly different regions of the world; Japan, Nepal, Panama, and the United States. Accounting for scale effects using the geomorphometric scaling relations increases transferability of TOPMODEL parameters form one catchment to another.

[55] The use of geomorphometric scaling of topographically derived parameters from a catchment in Japan to two catchments in Nepal, one catchment in Panama, and one catchment in the United States, demonstrates that the grid-resolution-dependent effective parametric value of lateral soil transmissivity T is quite stable from one place to another in the regionalization of TOPMODEL in humid catchments. Results indicate that the stability of the lateral transmissivity of soil requires that there should not be a scale mismatch between the parameter identification scale and model application scale, or topographic scaling relations should be applied to match the scales of model application and parameter identification. From the analysis made in the Town Brook catchment we observed that the transmissivity decay parameter m value is not dependent on the grid resolution. The values of m given by *Beven* [1997] do not seem to have any significant correlation with the other corresponding TOPMODEL parameter values. While there is a theoretical link between the exponential transmissivity profile and the recession curve, effectively m is most important in controlling the decay of the recession and hence values can be derived from recession analysis [*Ambroise et al.*, 1996]. This means that there will be a link between soil moisture storage capacity and catchment size rather than grid size. Larger catchments are more likely

to have longer-term storage. A prior estimate of the parameter m from the first-order hyperbolic function that fits the recession curve obtained from the observed discharge could be a good indication for the transferability of the m parameter value if data are available. The prior estimate of m obtained using the first-order hyperbolic function method for the two Nepalese catchments and the Upper Rio Chagres Panama, resulted in $m = 0.1$ and 0.06 respectively, which is close to the Kamishiiba-calibrated m value of 0.07. We recommend use of a prior estimate of the m parameter when the prior estimate significantly differs from the Kamishiiba value of 0.07, as was the case in our analysis of the Town Brook watershed data set.

[56] **Acknowledgments.** The authors thank Tammo Steenhuis and the City of New York, Department of Environmental Protection, for providing the Town Brook data. The Upper Rio Chagres Panama data were provided by Carlos Vargas, Jorge Espinosa, and Mike Hart of the Panama Canal Authority. The Balephi and Likhu data were provided by the Department of Hydrology and Meteorology, Government of Nepal. This research was supported in part by grant W911NF-07-1-0389 from the U. S. Army Research Office to the second author.

References

Ambroise, B., K. Beven, and J. Freer (1996), Towards a generalization of the TOPMODEL concepts: Topographic indices of hydrologic similarity, *Water Resour. Res.*, *32*, 2135–2145, doi:10.1029/95WR03716.

Andrle, R., and A. D. Abrahams (1989), Fractal techniques and the surface roughness of talus slopes, *Earth Surf. Processes Landforms*, *14*, 197–209, doi:10.1002/esp.3290140303.

Beven, K. (1995), Linking parameters across scales: Subgrid parameterizations and scale dependent hydrological models, in *Scale Issues in Hydrological Modelling*, edited by J. D. Kalma, and M. Sivapalan, pp. 263–281, John Wiley, Hoboken, N. J.

Beven, K. (1997), TOPMODEL: A critique, *Hydrol. Processes*, *11*, 1069–1085, doi:10.1002/(SICI)1099-1085(199707)11:9<1069::AID-HYP545>3.0.CO;2-O.

Beven, K. (2006), A manifesto for the equifinality thesis, *J. Hydrol.*, *320*, 18–36.

Beven, K. J., and M. J. Kirkby (1979), A physically based, variable contributing area model of basin hydrology, *Hydrol. Sci. Bull.*, *24*, 43–69.

Blöschl, G. (2005), Rainfall-runoff modeling of ungauged catchments, in *Encyclopedia of Hydrological Sciences*, edited by M. G. Anderson, pp. 1–19, John Wiley, Hoboken, N. J.

Brutsaert, W. (2008), Long-term groundwater storage trends estimated from streamflow records: Climatic perspective, *Water Resour. Res.*, *44*, W02409, doi:10.1029/2007WR006518.

Campling, P., A. Gobin, K. Beven, and J. Feyen (2002), Rainfall-runoff modelling of a humid tropical catchment: The TOPMODEL approach, *Hydrol. Processes*, *16*, 231–253, doi:10.1002/hyp.341.

Gyawali, D. (1989), *Water in Nepal*, 280 pp., Himal Books, Kathmandu.

Hannah, D. M., S. R. Kansakar, A. J. Gerrard, and G. Rees (2005), Flow regimes of Himalayan rivers of Nepal: Nature and spatial patterns, *J. Hydrol.*, *308*, 18–32, doi:10.1016/j.jhydrol.2004.10.018.

Harmon, R. S. (2005), An introduction to the Panama canal watershed, in *The Ñacute;o Chagres, Panama*, *Water Sci. Technol. Libr.*, vol. 52, edited by R. S. Harmon, pp. 19–28, Springer, New York.

Japan International Cooperation Agency (1985), *Master Plan Study of the Kosi River Water Resources Development*, Kathmandu.

Kavetski, D., G. Kuczera, and S. W. Franks (2003), Semidistributed hydrological modeling: A "saturation path" perspective on TOPMODEL and VIC, *Water Resour. Res.*, *39*(10), 1246, doi:10.1029/2003WR002122.

Kirkby, M. J. (1975), Hydrograph modeling strategies, in *Process in Physical and Human Geography*, edited by R. Peel, M. Chisholm, and P. Haggett, pp. 69–90, Elsevier, New York.

Klinkenberg, B., and M. F. Goodchild (1992), The fractal properties of topography: A comparison of methods, *Earth Surf. Processes Landforms*, *17*, 217–234, doi:10.1002/esp.3290170303.

Kuo, W., T. S. Steenhuis, C. E. McCulloch, C. L. Mohler, D. A. Weinstein, S. D. DeGloria, and D. P. Swaney (1999), Effect of grid size on runoff and soil moisture for a variable-source-area hydrology model, *Water Resour. Res.*, *35*(11), 3419–3428, doi:10.1029/1999WR900183.

Lyon, S. W., M. T. Walter, P. Gérard-Marchant, and T. S. Steenhuis (2004), Using a topographic index to distribute variable source area runoff predicted with the SCS curve-number equation, *Hydrol. Processes*, *18*, 2757–2771, doi:10.1002/hyp.1494.

Molicova, H., M. Grimaldi, M. Bonell, and P. Hubert (1997), Using TOPMODEL towards identifying and modelling the hydrological patterns within a headwater tropical catchment, *Hydrol. Processes*, *11*, 1169–1196, doi:10.1002/(SICI)1099-1085(199707)11:9<1169::AID-HYP551>3.0.CO;2-W.

Nayava, J. L. (1980), Rainfall in Nepal, *Himalayan Rev*, *12*, 1–18.

Niedzialek, J. M., and F. L. Ogden (2005), Runoff production in the Upper Ñacute;o Chagres watershed, Panama, in *The Ñacute;o Chagres*, *Panama*, *Water Sci. Technol. Libr.*, vol. 52, edited by R. S. Harmon, pp. 149–168, Springer, New York.

Nimmo, J. R. (2007), Simple predictions of maximum transport rate in unsaturated soil and rock, *Water Resour. Res.*, *43*, W05426, doi:10.1029/2006WR005372.

Parajka, J., R. Merz, and G. Bloschl (2005), A comparison of regionalization methods for catchment model parameters, *Hydrol. Earth Syst. Sci.*, *9*, 157–171.

Pilgrim, D. H. (1983), Some problems in transferring hydrological relationships between small and large drainage basins and between regions, *J. Hydrol.*, *65*, 49–72, doi:10.1016/0022-1694(83)90210-X.

Pradhan, N. R., Y. Tachikawa, and K. Takara (2006), A downscaling method of topographic index distribution for matching the scales of model application and parameter identification, *Hydrol. Processes*, *20*, 1385–1405, doi:10.1002/hyp.6098.

Steenhuis, T. S., M. Winchell, J. Rossing, J. A. Zollweg, and M. F. Walter (1995), SCS runoff equation revisited for variable-source runoff areas, *J. Irrig. Drain. Eng.*, *121*, 234–238, doi:10.1061/(ASCE)0733-9437(1995)121:3(234).

Vázquez, R. F., J. Feyen, and J. C. Refsgaard (2002), Effect of grid size on effective parameters and model performance of the MIKE-SHE code, *Hydrol. Processes*, *16*, 355–372, doi:10.1002/hyp.334.

Ward, R. C. (1984), On the response to precipitation of headwater streams in humid areas, *J. Hydrol.*, *74*, 171–189, doi:10.1016/0022-1694(84)90147-1.

Zhang, W., and D. R. Montgomery (1994), Digital elevation model grid size, landscape representation, and hydrologic simulations, *Water Resour. Res.*, *30*, 1019–1028, doi:10.1029/93WR03553.

F. L. Ogden and N. R. Pradhan, Department of Civil and Architectural Engineering, University of Wyoming, Laramie, WY 82071, USA. (fogden@uwyo.edu; nawa_water@yahoo.com)

Y. Tachikawa, Hydrology and Water Resources Engineering Laboratory, Department of Urban and Environmental Engineering, Kyoto University, Kyoto 615-8540, Japan. (tachikawa@mbox.kudpc.kyoto-u.ac.jp)

K. Takara, Disaster Prevention Research Institute, Kyoto University, Kyoto 611-0011, Japan. (takara@mbox.kudpc.kyoto-u.ac.jp)